Recording of leg movements and flight steering

Stance–swing movements of a front leg during walking (Fig. 1b) or the lateral steering movements of the abdomen[20] during flight (Fig. 2e) were measured with an optoelectronic camera[27]. A piece of reflective disc (3M, Scotchlite 7610) was attached to the femur or abdomen and illuminated. The reflected light was picked up by a position-sensitive photodiode and indicated the position of the body part. For measurements during flight, crickets were tethered by their pins in front of a constant air stream to elicit flying. Conditions of acoustic stimulation were otherwise identical to the trackball experiments.

Received 13 May; accepted 25 June 2004; doi:10.1038/nature02787.

1. Webster, D. B., Fay, R. R. & Popper, A. N. *The Evolutionary Biology of Hearing* (Springer, Berlin, New York, 1992).
2. Pollack, G. S. Analysis of temporal patterns of communication signals. *Curr. Opin. Neurobiol.* **11,** 734–738 (2001).
3. Balakrishnan, R., von Helversen, D. & von Helversen, O. Song pattern recognition in the grasshopper *Chorthippus biguttulus*: the mechanism of syllable onset and offset detection. *J. Comp. Physiol. A* **187,** 255–264 (2001).
4. Weber, T. & Thorson, J. in *Cricket Behaviour and Neurobiology* (eds Huber, F., Moore, T. E. & Loher, W.) 310–339 (Cornell Univ. Press, Ithaca, London, 1989).
5. Hoy, R. R. Acoustic communication in crickets: a model system of feature detection. *Fed. Proc.* **37,** 2316–2323 (1978).
6. Schildberger, K. Temporal selectivity of identified auditory neurons in the cricket brain. *J. Comp. Physiol. A* **155,** 171–185 (1984).
7. Hennig, R. M. Acoustic feature extraction by cross correlation in crickets? *J. Comp. Physiol. A* **189,** 589–598 (2003).
8. Pollack, G. S. Discrimination of calling song models by the cricket, *Teleogryllus oceanicus*: the influence of sound direction on neural encoding of the stimulus temporal pattern and on phonotactic behaviour. *J. Comp. Physiol. A* **158,** 549–561 (1986).
9. Stabel, J., Wendler, G. & Scharstein, H. Cricket phonotaxis: localization depends on recognition of the calling song pattern. *J. Comp. Physiol. A* **165,** 165–177 (1989).
10. von Helversen, D. & von Helversen, O. Acoustic pattern recognition and orientation in orthopteran insects: parallel or serial processing? *J. Comp. Physiol. A* **177,** 767–774 (1995).
11. Webb, B. Robots in invertebrate neuroscience. *Nature* **417,** 359–363 (2002).
12. Webb, B. & Scutt, T. A simple latency-dependent spiking-neuron model of cricket phonotaxis. *Biol. Cybern.* **82,** 247–269 (2000).
13. Arkin, R. C. *Behaviour-Based Robotics* (MIT, Cambridge, London, 1998).
14. Gerhard, H. C. & Huber, F. *Acoustic Communication in Insects and Anurans* (Univ. of Chicago Press, Chicago and London, 2002).
15. Huber, F. Cricket neuroethology: neuronal basis of intraspecific acoustic communication. *Adv. Study Behav.* **19,** 299–356 (1990).
16. Pollack, G. S. Who, what, where? Recognition and localization of acoustic signals by insects. *Curr. Opin. Neurobiol.* **10,** 763–767 (2000).
17. Popov, A. V. & Shuvalov, V. F. Phonotactic behaviour of crickets. *J. Comp. Physiol. A* **119,** 111–126 (1977).
18. Doherty, J. A. Temperature coupling and trade-off phenomena in the acoustic communication system of the cricket, *Gryllus bimaculatus* de Geer (Gryllidae). *J. Exp. Biol.* **114,** 17–35 (1985).
19. Murphey, R. K. & Zaretsky, M. D. Orientation to calling song by female crickets, *Scasipedus marginatus* (Gryllidae). *J. Exp. Biol.* **56,** 335–352 (1972).
20. Ulagarai, S. M. & Walker, T. J. Phonotaxis of crickets in flight: attraction of male and female crickets to male calling songs. *Science* **182,** 1278–1279 (1973).
21. Moiseff, A., Pollack, G. S. & Hoy, R. R. Steering responses of flying crickets to sound and ultrasound: mate attraction and predator avoidance. *Proc. Natl Acad. Sci. USA* **75,** 4052–4056 (1978).
22. Schildberger, K., Huber, F. & Wohlers, D. W. in *Cricket Behaviour and Neurobiology* (eds Huber, F., Moore, T. E. & Loher, W.) 423–458 (Cornell Univ. Press, Ithaca, London, 1989).
23. Weber, T., Thorson, J. & Huber, F. Auditory behaviour of the cricket. I: Dynamics of compensated walking and discrimination paradigms on the Kramer treadmill. *J. Comp. Physiol. A* **141,** 215–232 (1981).
24. Schmitz, B., Scharstein, H. & Wendler, G. Phonotaxis in *Gryllus campestris* L. (Orthoptera, Gryllidae). I: Mechanism of acoustic orientation in intact female crickets. *J. Comp. Physiol. A* **148,** 431–444 (1982).
25. Doherty, J. A. Song recognition and localization in the phonotaxis behavior of the field cricket, *Gryllus bimaculatus* (Orthoptera: Gryllidae). *J. Comp. Physiol. A* **168,** 213–222 (1991).
26. Weber, T. & Thorson, J. Auditory behaviour of the cricket. IV: Interaction of direction of tracking with perceived split-song paradigms. *J. Comp. Physiol. A* **163,** 13–22 (1988).
27. Hedwig, B. A highly sensitive opto-electronic system for the measurement of movements. *J. Neurosci. Methods* **100,** 165–171 (2000).
28. Pollack, G. S. & Hoy, R. R. Phonotaxis in flying crickets: neural correlates. *J. Insect Physiol.* **27,** 41–45 (1981).
29. Nabatiyan, A., Poulet, J. F. A., de Polavieja, G. G. & Hedwig, B. Temporal pattern recognition based on instantaneous spike rate coding in a simple auditory system. *J. Neurophysiol.* **90,** 2484–2493 (2003).
30. Cade, W. H. Effect of male deprivation on female phonotaxis in field crickets (Orthoptera: Gryllidae; *Gryllus*). *Can. Entomol.* **111,** 741–744 (1979).

Acknowledgements We thank our Cambridge and Edinburgh colleagues for comments on the manuscript. The BBSRC and the Royal Society supported the project. We are grateful to M. Knepper and P. Williams for the development of software and hardware and to Röhm GmbH for providing Rohacell.

Competing interests statement The authors declare that they have no competing financial interests.

Correspondence and requests for materials should be addressed to B.H. (bh202@cam.ac.uk) or J.F.A.P. (jfap2@cam.ac.uk).

MicroRNAs act sequentially and asymmetrically to control chemosensory laterality in the nematode

Sarah Chang[1], Robert J. Johnston Jr[1], Christian Frøkjær-Jensen[2], Shawn Lockery[2] & Oliver Hobert[1]

[1]*Department of Biochemistry and Molecular Biophysics, Center for Neurobiology and Behavior, Columbia University Medical Center, 701 W. 168th Street, New York 10032, USA*

[2]*Institute of Neuroscience, University of Oregon, Eugene, Oregon 97403, USA*

Animal microRNAs (miRNAs) are gene regulatory factors that prevent the expression of specific messenger RNA targets by binding to their 3′ untranslated region[1–3]. The *Caenorhabditis elegans lsy-6* miRNA (for lateral symmetry defective) is required for the left/right asymmetric expression of guanyl cyclase (*gcy*) genes in two chemosensory neurons termed ASE left (ASEL) and ASE right (ASER)[4,5]. The asymmetric expression of these putative chemoreceptors in turn correlates with the functional lateralization of the ASE neurons[6]. Here we find that a mutation in the *die-1* zinc-finger transcription factor disrupts both the chemosensory laterality and left/right asymmetric expression of chemoreceptor genes in the ASE neurons. *die-1* controls chemosensory laterality by activating the expression of *lsy-6* specifically in ASEL, but not in ASER, where *die-1* expression is downregulated through two sites in its 3′ untranslated region. These two sites are complementary to *mir-273*, a previously uncharacterized miRNA, whose expression is strongly biased towards ASER. Forced bilateral expression of *mir-273* in ASEL and ASER causes a loss of asymmetric *die-1* expression and ASE laterality. Thus, an inverse distribution of two sequentially acting miRNAs in two bilaterally symmetric neurons controls laterality of the nematode chemosensory system.

Although miRNAs are abundant in animal genomes, the biological contexts and pathways in which miRNAs operate are only beginning to be explored[3]. The *C. elegans lsy-6* miRNA functions in a poorly understood developmental context, the generation of neuronal diversity along the left/right axis of an animal[4,5]. *lsy-6* superimposes a left/right asymmetric expression profile of putative chemosensory receptors, encoded by the *gcy* genes, onto the bilaterally symmetric differentiation program of two chemosensory neurons, ASEL and ASER[4,5]. Asymmetric *gcy* chemoreceptor expression in turn correlates with the left/right asymmetric chemosensory capacities of ASEL and ASER[6]. An essential prerequisite for ASEL/R laterality is the restriction of *lsy-6* expression to the ASEL neuron[5].

To gain a better mechanistic understanding of *lsy-6*-mediated lateralization of the ASE neurons, we conducted genetic screens for mutants that show defects in asymmetric expression of ASE-specific putative *gcy* chemoreceptors (see Supplementary Information)[7]. One of the alleles retrieved from this screen, *ot26*, showed a 100% penetrant *lsy* phenotype in adult animals; both ASE cells expressed the normally ASER-specific *gcy-5* gene and concomitantly lost the expression of the normally ASEL-specific *gcy-7* gene (Fig. 1a, b). The expression of several cell-fate markers that label bilaterally symmetric aspects of ASEL/R differentiation were unaffected (data not shown).

Further analysis of *ot26* mutants showed that the laterality defects at the genetic level were tightly correlated with defects at the behavioural level. Previous studies of chemotaxis behaviour in worms, in which either the left or right ASE neuron was killed,

indicated that ASEL and ASER are functionally distinct; ASEL responds strongly to Na^+ ions, and not at all to Cl^- ions, whereas ASER responds strongly to Cl^- ions, but only weakly to Na^+ ions (Fig. 1c; wild-type-model)[6]. Given that in *ot26* mutants, ASEL seems to adopt an ASER-specific chemoreceptor expression profile (Fig. 1b), *ot26* mutants might be expected to behave as though they have two ASER neurons (Fig. 1c, 2-ASER model). If so, chemotaxis to Na^+ ions, which are a weaker stimulus for ASER, should be impaired, whereas chemotaxis to Cl^- ions should be intact or even enhanced. As predicted by the 2-ASER model, *ot26* mutants were indeed defective in locating the peak of a gradient of Na^+ ions, especially in the presence of a high, uniform concentration of Cl^- ions (Fig. 1d, e). Furthermore, *ot26* mutants were better at finding the peak of a gradient of Cl^- ions in the presence of a high, uniform concentration of Na^+ ions (Fig. 1f). Therefore, the *ot26* allele affects a gene that is necessary for forming distinct neuronal representations of chemosensory inputs.

Single-nucleotide-polymorphism mapping, complementation testing, transformation rescue and allele sequencing showed that *ot26* is an allele of the *die-1* gene (Supplementary Fig. 1a). The *die-1* gene encodes a C2H2 zinc-finger transcription factor previously implicated in hypodermal patterning[8]. Other *die-1* alleles show similar lateralization defects (Supplementary Fig. 1a). A *die−1^{resc} :: gfp* reporter gene, which rescues the *lsy* defect (Supplementary Fig. 1b), shows a dynamic expression profile with early hypodermal expression ceasing at gastrulation and then reappearing in late embryos in several putative head neurons[8]. Using an ASE-neuron-expressed red-fluorescent-protein reporter (*ceh-36^{prom}::rfp*), we identified two of these neurons as ASEL and ASER. However, expression is strongly biased towards ASEL (Fig. 2a). We corroborated the autonomous function of *die-1* in the mature ASEL neurons by expressing the *die-1* complementary DNA under the control of the promoter of the ASEL-specific *gcy-7* gene. When expressed in a *die-1* mutant background, three of four lines showed rescue of the *lsy* phenotype (Supplementary Fig. 1b).

We previously described a pathway consisting of several gene-regulatory factors that controls left/right asymmetric *gcy* gene expression in ASEL/R (summarized in Fig. 4)[7]. Placing *die-1* into this pathway, we found a completely penetrant loss of *lim-6* homeobox gene expression in adult *die-1(ot26)* mutant animals (Supplementary Fig. 2). Because correct *lim-6* expression requires the tightly regulated balance of the *ceh-36* activator homeobox gene and the *cog-1* repressor homeobox gene (Fig. 4)[7], a loss of *lim-6* expression is consistent with either a decrease in the expression of the *ceh-36* activator or an increase in the expression of the *cog-1* repressor. We found that loss of *die-1* had no effect on *ceh-36* expression ($n = 52$), but instead caused a strong de-repression of *cog-1::gfp* expression in ASEL (Fig. 2b). Furthermore, expressing *die-1* ectopically in the ASER neuron demonstrated that *die-1* is not only necessary but also sufficient to repress *cog-1* expression (Fig. 2b).

One possible explanation for the ability of *die-1* to repress *cog-1* expression is that *die-1* regulates expression of *lsy-6*, a miRNA that we previously have shown to inhibit *cog-1* expression through

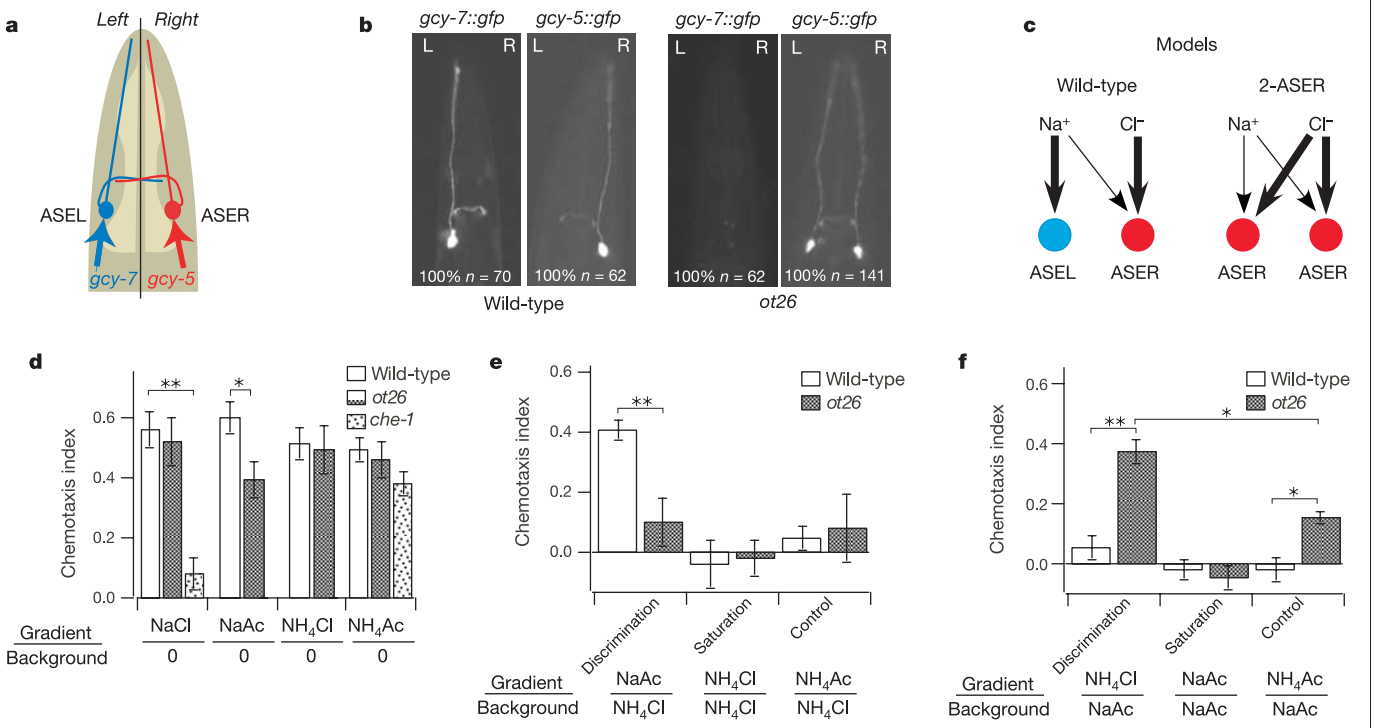

Figure 1 Laterality of ASE neurons is disrupted in *ot26* mutant animals. **a**, Schematic structure of ASEL/R and *gcy* gene expression profiles[16]. **b**, Transgenic adult animals expressing *gcy-5^{prom}::gfp (ntIs1)* or *gcy-7^{prom}::gfp (otIs3)* in wild-type or *ot26* mutant backgrounds. **c**, Models of chemosensory processing in ASEL/R neurons of wild-type and *ot26* (2-ASER) animals. Arrow thickness represents relative sensitivity to the indicated ion, inferred from laser-ablation experiments[6]. Na^+ versus Cl^- sensitivity in the 2-ASER model predicts reduced Na^+ chemotaxis and normal or enhanced Cl^- chemotaxis for these ions tested alone (**d**), defective Na^+ versus Cl^- discrimination (**e**, 'Discrimination'), and normal or enhanced Cl^- versus Na^+ discrimination (**f**, 'Discrimination'). **d–f**, Average chemotaxis index of wild-type and *ot26* animals in chemotaxis assays and discrimination tests. The composition of the chemical gradient that was superimposed upon the background stimulus (if any) is shown below each pair of bars. Peak concentration of the gradients was ~10 mM; background concentrations were 100 mM. Bars are mean ± s.e.; three to nine assays per datum (bar) with $N > 100$ animals per assay. Asterisks indicate significance at $P < 0.05$ (*) and $P < 0.01$ (**). All strains contained the *ntIs1 (gcy-5^{prom}::gfp)* transgene in the background. For counter-ions (NH_4 and Ac) and controls (*che-1*) see Supplementary Information. Relative chemotaxis performance of wild-type worms and *ot26* mutants was consistent with the predictions in **c**. The enhanced response of *ot26* mutants to an NH_4Ac gradient (**f**, 'Control') is significantly weaker than the enhanced NH_4Cl response (**f**, 'Discrimination'), confirming the Cl^- specificity of the latter.

binding to its 3′ untranslated region (UTR)[4]. In support of this, we found that *lsy-6* expression in ASEL is abolished in a *die-1* mutant background (Fig. 2c). In other neurons, *die-1* has no effect on *lsy-6* expression, illustrating that the promoter of the *lsy-6* locus samples distinct transcriptional regulatory inputs in different cell types. In the context of the ASE neurons, *die-1* is not only necessary but also sufficient to control *lsy-6* expression, because ectopic expression of *die-1* in ASER results in ectopic *lsy-6*^{prom}*::gfp* expression (Fig. 2c). We confirmed that *die-1* acts through *lsy-6* to repress *cog-1* expression by demonstrating that transgenic animals that express *die-1* in ASER are not able to turn off *cog-1* expression in a *lsy-6* null mutant background (Fig. 2b).

We next investigated how *die-1* and hence *lsy-6* activation is spatially biased towards ASEL. Because the inverse asymmetry of *cog-1* expression in this regulatory cascade (ASER > ASEL expression) is controlled by *lsy-6* binding to the *cog-1* 3′ UTR, we asked whether *die-1* expression is also controlled by its 3′ UTR. To test this idea, we constructed a 'sensor gene' in which *gfp* transcripts were produced under the control of the *ceh-36* promoter in both ASEL and ASER. When *gfp* transcripts are fused to a heterologous 3′ UTR, GFP expression is observed in ASEL and ASER at a comparable level (Fig. 3a)[4,7]. If the transcript is fused to the 3′ UTR of the *cog-1* gene, which is responsive to the ASEL-expressed *lsy-6* miRNA, downregulation of GFP expression is observed in ASEL[4]. If the *gfp* transcript is fused to the 3′ UTR of the *die-1* gene, GFP expression is significantly downregulated in ASER (Fig. 3a). The 3′ UTR of *die-1* therefore contains elements that are subject to left/right-specific control of expression, providing a mirror image of control-of-expression of the *cog-1* 3′ UTR.

We next sought to identify a miRNA that may control *die-1* expression through binding to the 3′ UTR of *die-1*. Using an approach conceptually similar to 'phylogenetic footprinting' (traditionally used to identify transcription-factor binding sites in putative transcriptional regulatory regions[9]), we compared the 3′ UTRs of the *die-1* gene from *C. elegans* with those from the related nematode, *Caenorhabditis briggsae*. We found three phylogenetic footprints with consecutive stretches of >10-nucleotide sequence identity in the respective *die-1* 3′ UTRs (Supplementary Fig. 3a). When these were translated into RNA, we noted that two of the sites each showed complementarity to a hypothetical stretch of six nucleotides, 3′–UG(C/U)(C/U)(C/U)G–5′ (Supplementary Fig. 3a). We inferred that this stretch of six nucleotides is a part of

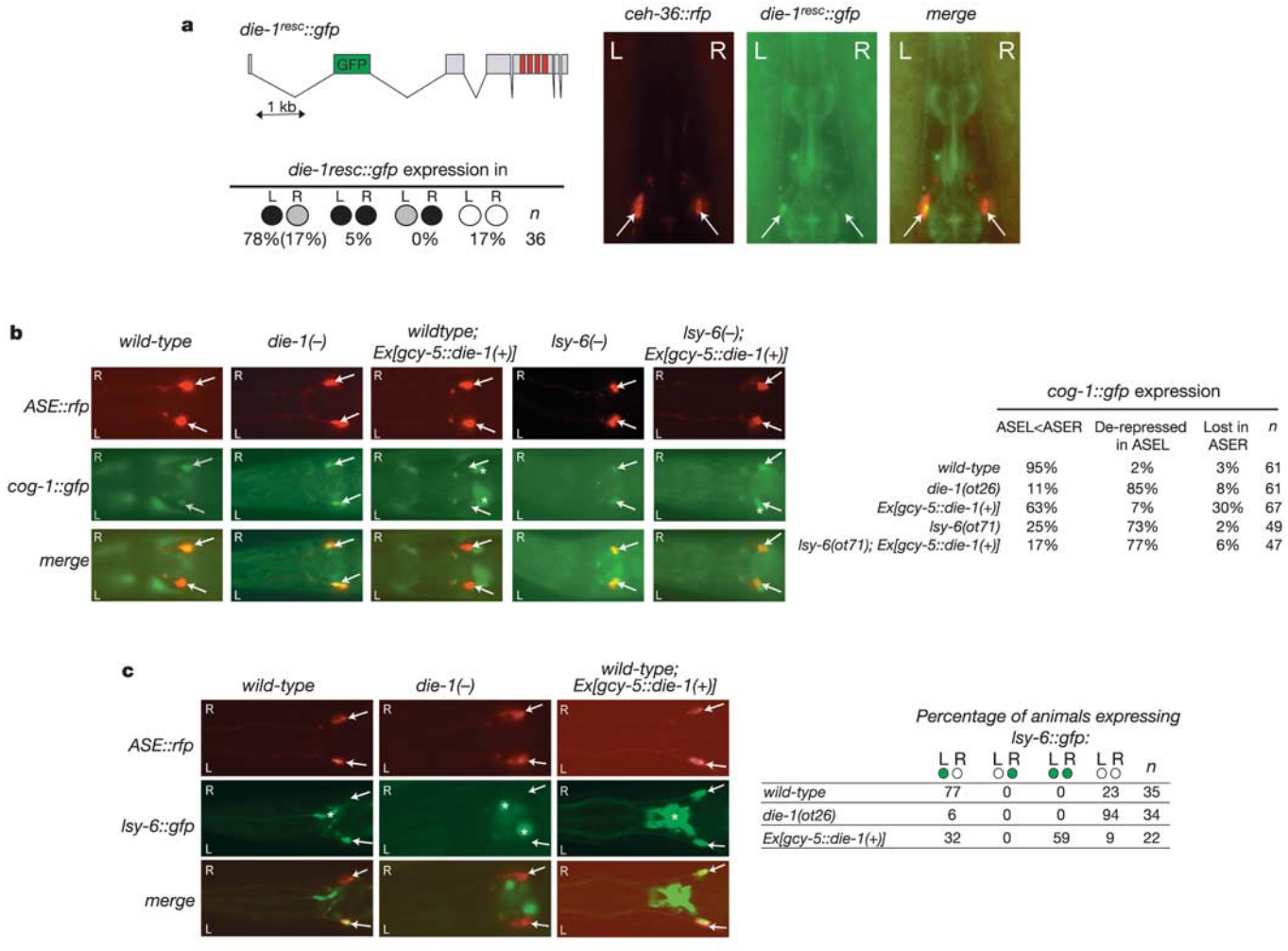

cog-1::gfp expression

	ASEL<ASER	De-repressed in ASEL	Lost in ASER	*n*
wild-type	95%	2%	3%	61
die-1(ot26)	11%	85%	8%	61
Ex[gcy-5::die-1(+)]	63%	7%	30%	67
lsy-6(ot71)	25%	73%	2%	49
lsy-6(ot71); Ex[gcy-5::die-1(+)]	17%	77%	6%	47

Percentage of animals expressing lsy-6::gfp:

	L R ●○	L R ○●	L R ●●	L R ○○	*n*
wild-type	77	0	0	23	35
die-1(ot26)	6	0	0	94	34
Ex[gcy-5::die-1(+)]	32	0	59	9	22

Figure 2 The zinc-finger transcription factor, DIE-1, is predominantly expressed in ASEL and affects *lsy-6* expression. **a**, Expression pattern of a chromosomally integrated *die-1*^{resc}*::gfp* reporter construct (*otIs159*). ASE cells were identified with the *otIs151 (ceh36*^{prom}*::rfp)* array. See Supplementary Information for more details on expression patterns and constructs. Circles indicate expression levels. Number in parenthesis indicates expression exclusively in ASEL. **b**, *cog-1* expression in various genetic backgrounds, monitored with the *sylS63* array, which contains the complete *cog-1* locus[17]. ASEL/R (shown by arrows) were identified with a *ceh-36*^{prom}*::rfp* transgene, which is also expressed in the AWC neurons. Asterisks point to other *cog-1::gfp* expressing cells. The tabular data quantify the expression levels (some animals appear in more than one category). **c**, Expression of *lsy-6*^{prom}*::gfp (otEx1403)* in wild-type (left panels), in *die-1(ot26)* mutant animals (middle panels) and transgenic wild-type animals that express *die-1* in ASER (*otEx1192* array) (left panels). Asterisks point to other *lsy-6*^{prom}*::gfp*-expressing cells.

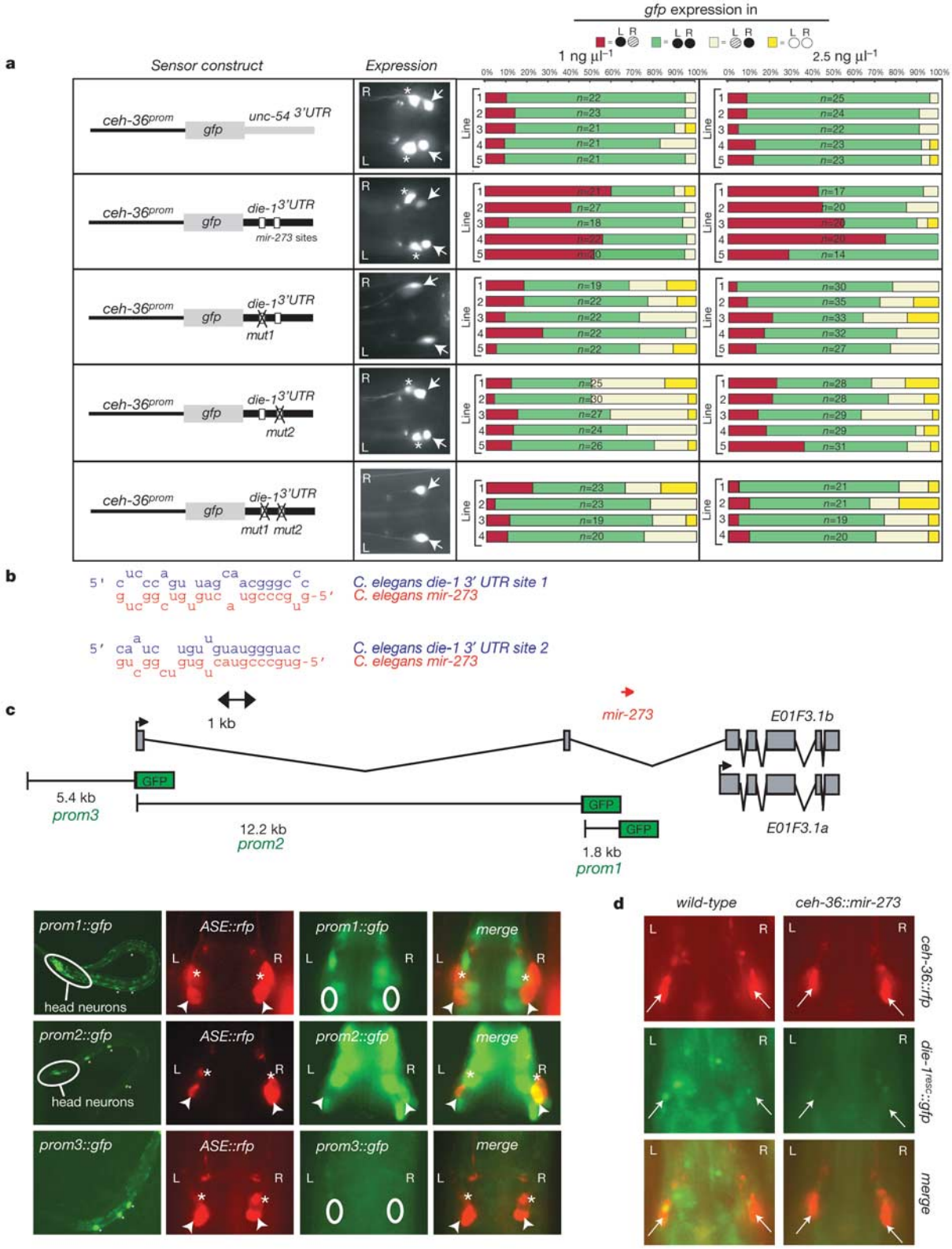

Figure 3 *die-1* regulation by the *mir-273* miRNA. **a**, Expression of *die-1* $^{3'\ UTR}$ sensor constructs in ASEL and ASER. In 'mut1' the 'acgggc' core of the the *mir-273* complementary site is changed to 'guaacu'; in 'mut2' the 'gggua' core is changed to 'cuacg'. Sensor constructs were injected at two different concentrations as indicated. **b**, Complementarity of *die-1* 3′ UTR sites and *mir-273*. **c**, *mir-273* expression pattern deduced from reporter gene fusions. *prom1* and *prom2* are exclusively expressed in head neurons; *prom2* shows biased expression in the ASER neuron (for quantification, see Supplementary Table 1). Several transgenic lines show similar expression patterns. *ceh-36* ^{prom}*::rfp* (*otIs151*) identifies ASEL and ASER. Asterisks in left panels indicate cells that fluoresce owing to the injection marker used (*unc-122* ^{prom}*::gfp*); asterisks in other panels indicate AWC neurons. **d**, Bilateral expression of *mir-273* (*ceh-36* ^{prom}*::mir-273; otEx1705*) disrupts *die-1* expression, assayed with the *otIs159 (die-1* ^{resc}*::gfp)* transgene (for quantification, see Supplementary Table 2).

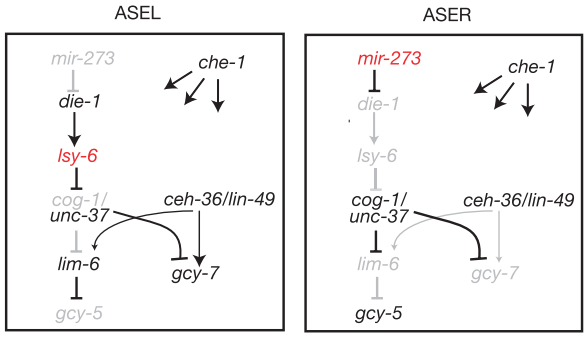

Figure 4 Gene regulatory cascade in ASEL and ASER. Genetic data from this paper and refs 4 and 7 are summarized. miRNAs acting in this cascade are indicated in red.

a miRNA that exerts control over the 3′ UTR. We examined the sequences of all predicted miRNAs in the *C. elegans* genome (http://www.sanger.ac.uk/Software/Rfam/mirna/) and found a match for this sequence in the functionally uncharacterized *mir-273* miRNA (Supplementary Fig. 3b)[10]. The complementarity of *mir-273* to the two phylogenetic footprints in the *die-1* 3′ UTR extends to a total of 19–21 nucleotides (Fig. 3b), a common length of miRNA/target duplexes[1–3,11]. As expected from the conserved nature of the six-nucleotide sequence with which we conducted the search, this sequence lies at the 5′ end of *mir-273* (Fig. 3b), where most known miRNAs show the highest degree of sequence identity to their target sites[11]. To investigate whether the 3′ UTR-mediated downregulation of *die-1* expression depends on the two *mir-273*-complementary sites, we mutated each of the sites in the sensor *gfp* construct. Each of the mutant sensor constructs failed to be downregulated in ASER (Fig. 3a). The requirement for each complementary site is consistent with the previously observed cooperativity of miRNA action[12].

The downregulation of the *die-1* 3′ UTR in a manner that is (1) dependent on the *mir-273* complementary sites, and (2) specific to the ASER cell, suggests that *mir-273* activity is biased towards ASER, possibly through left/right differential gene expression. Using *gfp* reporter constructs that sample potential transcriptional *cis*-regulatory inputs into the *mir-273* locus, we inferred that *mir-273* is expressed in several bilaterally symmetric pairs of head neurons (Fig. 3c). Left/right asymmetric expression was indeed observed in the ASE neurons, with expression in ASER being significantly higher than in ASEL (Fig. 3c; Supplementary Table 1). If the asymmetric distribution of *mir-273* was functionally relevant, we would expect that forced, symmetric expression of *mir-273* in both ASEL and ASER would repress *die-1* expression and hence disrupt ASE laterality. Indeed, transgenic animals that express *mir-273* from the bilateral *ceh-36* promoter (*ceh-36*^{prom}*::mir-273*) not only show a downregulation of *die-1*^{resc}*::gfp* expression (Fig. 3d), but also show the 2-ASER chemoreceptor profile that is characteristic of the *die-1* loss-of-function phenotype (Supplementary Fig. 4). Diametrically opposite effects (2-ASEL phenotype) can be observed if the normally left-side-specific miRNA *lsy-6* is expressed under control of the bilateral *ceh-36* promoter[4].

Starting with the identification of a mutant strain that shows laterality defects both in gene expression patterns and in functional capacities, we have described a critical transcription factor component of a gene regulatory cascade that controls left/right asymmetry in the chemosensory system of *C. elegans*. This cascade uses several fundamental principles of gene regulation, one being the use of a series of sequential repressive interactions[13], another being the extensive use of miRNA-mediated control of gene expression (Fig. 4). The spatial restriction of the expression of one of the miRNAs involved in this pathway, *lsy-6*, is controlled through another spatially controlled miRNA, *mir-273*. This regulatory effect is mediated by the *die-1* zinc-finger transcription factor, the first transcription factor found to confer spatial control of animal miRNA gene expression. Therefore, ASEL and ASER show reciprocal miRNA expression profiles, an essential requirement for determining laterality of the chemosensory system. □

Methods

Strains, genetic screening and mapping

A detailed list of strains and genetic approaches can be found in the Supplementary Information.

DNA constructs and transgenes

A *die-1*-rescuing *gfp* plasmid (pPH12, '*die-1*^{resc}*::gfp*') was provided by J. Hardin (see Supplementary Information)[8]. Polymerase chain reaction (PCR) fusion[14] was used to generate *mir-273* promoter fusion constructs and 3′ UTR sensor constructs. For the latter, five kilobases (kb) of the *ceh-36* promoter were PCR-fused to *gfp* coding sequences and then, in a second PCR fusion reaction, fused to an *unc-54*$^{3'\ UTR}$ or the *die-1*$^{3'\ UTR}$-PCR amplicon. To generate the mutated sensor constructs, the *die-1*$^{3'\ UTR}$ was amplified with a total of four PCR primers that harbour the mutated *mir-273* complementary sites. To generate *gcy-5*^{prom}*::die-1* and *gcy-7*^{prom}*::die-1, gfp* from *gcy-5Hind::gfp* and *gcy-7Hind::gfp* expression constructs[7] was replaced with a *die-1* cDNA (provided by J. Hardin). PCR fusion was used to generate *mir-273* misexpression constructs, using the 5-kb *ceh-36* promoter and the predicted 94-base pair (bp) *mir-273* hairpin. See Supplementary Information for PCR primer sequences used for PCR fusions. Transgenic lines were usually generated in a wild-type (strain N2) background using *unc-122*^{prom}*::gfp* (50 ng μl^{-1}) or *rol-6* (100 ng μl^{-1}) as injection markers.

Chemotaxis assays

Radial gradient assays were based on previously described assays[15]. A detailed description can be found in the Supplementary Information.

Received 17 March; accepted 14 June 2004; doi:10.1038/nature02752.

1. Lee, R. C., Feinbaum, R. L. & Ambros, V. The *C. elegans* heterochronic gene *lin-4* encodes small RNAs with antisense complementarity to *lin-14*. *Cell* **75,** 843–854 (1993).
2. Wightman, B., Ha, I. & Ruvkun, G. Post-transcriptional regulation of the heterochronic gene *lin-14* by *lin-4* mediates temporal pattern formation in *C. elegans*. *Cell* **75,** 855–862 (1993).
3. Bartel, D. P. MicroRNAs: genomics, biogenesis, mechanism, and function. *Cell* **116,** 281–297 (2004).
4. Johnston, R. J. & Hobert, O. A microRNA controlling left/right neuronal asymmetry in *Caenorhabditis elegans*. *Nature* **426,** 845–849 (2003).
5. Hobert, O., Johnston, R. J. Jr & Chang, S. Left-right asymmetry in the nervous system: the *Caenorhabditis elegans* model. *Nature Rev. Neurosci.* **3,** 629–640 (2002).
6. Pierce-Shimomura, J. T., Faumont, S., Gaston, M. R., Pearson, B. J. & Lockery, S. R. The homeobox gene *lim-6* is required for distinct chemosensory representations in *C. elegans*. *Nature* **410,** 694–698 (2001).
7. Chang, S., Johnston, R. J. Jr & Hobert, O. A transcriptional regulatory cascade that controls left/right asymmetry in chemosensory neurons of *C. elegans*. *Genes Dev.* **17,** 2123–2137 (2003).
8. Heid, P. J. *et al.* The zinc-finger protein DIE-1 is required for late events during epithelial cell rearrangement in *C. elegans*. *Dev. Biol.* **236,** 165–180 (2001).
9. Bulyk, M. L. Computational prediction of transcription-factor binding site locations. *Genome Biol.* **5,** 201 (2003).
10. Grad, Y. *et al.* Computational and experimental identification of *C. elegans* microRNAs. *Mol. Cell.* **11,** 1253–1263 (2003).
11. Stark, A., Brennecke, J., Russell, R. B. & Cohen, S. M. Identification of *Drosophila* microRNA targets. *PLoS Biol.* **1,** 1–13 (2003).
12. Doench, J. G., Petersen, C. P. & Sharp, P. A. siRNAs can function as miRNAs. *Genes Dev.* **17,** 438–442 (2003).
13. Muhr, J., Andersson, E., Persson, M., Jessell, T. M. & Ericson, J. Groucho-mediated transcriptional repression establishes progenitor cell pattern and neuronal fate in the ventral neural tube. *Cell* **104,** 861–873 (2001).
14. Hobert, O. PCR fusion-based approach to create reporter gene constructs for expression analysis in transgenic *C. elegans*. *Biotechniques* **32,** 728–730 (2002).
15. Bargmann, C. I. & Horvitz, H. R. Chemosensory neurons with overlapping functions direct chemotaxis to multiple chemicals in *C. elegans*. *Neuron* **7,** 729–742 (1991).
16. Yu, S., Avery, L., Baude, E. & Garbers, D. L. Guanylyl cyclase expression in specific sensory neurons: a new family of chemosensory receptors. *Proc. Natl Acad. Sci. USA* **94,** 3384–3387 (1997).
17. Palmer, R. E., Inoue, T., Sherwood, D. R., Jiang, L. I. & Sternberg, P. W. *Caenorhabditis elegans* cog-1 locus encodes GTX/Nkx6.1 homeodomain proteins and regulates multiple aspects of reproductive system development. *Dev. Biol.* **252,** 202–213 (2002).

Supplementary Information accompanies the paper on **www.nature.com/nature**.

Acknowledgements We thank C. Antonio for the *ot100* allele, J.Hardin for *die-1* reagents, Q. Chen and S. Narula for expert technical assistance, J. Tien for help with mapping *ot26*, I. Greenwald for advice, L. Johnston, A. Lanjuin, P. Sengupta, I. Greenwald and F. Slack for reading the manuscript. S.C. was funded by an NIH predoctoral fellowship, R.J.J. by an NSF predoctoral fellowship, and C.F.-J. by a American Heart Association predoctoral fellowship. O.H. was supported by grants from the NIH, the McKnight Foundation and the Irma T.Hirschl Trust.

Competing interests statement The authors declare that they have no competing financial interests.

Correspondence and requests for materials should be addressed to O.H. (or38@columbia.edu)